(33)

N90-17949

THE AUSTRALIAN EXPERIMENT WITH ETS-V

Wolfhard J. Vogel, Julius Goldhirsh, Yoshihiro Hase+

EERL	APL	CRL
Univ. of Texas	Johns Hopkins Univ.	Ministry of P&T
Austin, TX	Laurel, MD	Kashima, Japan

Abstract--Land-mobile-satellite propagation measurements were implemented at L Band (1.5 GHz) in South-Eastern Australia during an 11 day period in October 1988. Transmissions (CW) from both the Japanese ETS-V and INMARSAT Pacific geostationary satellites were accessed. Previous measurements in this series were performed at both L Band (1.5 GHz) and UHF (870 MHz) in Central Maryland, North-Central Colorado, and the southern United States. The objectives of the Australian campaign were to expand the data base acquired in the U.S. to another continent, to validate a U.S. derived empirical model for estimating the fade distribution, to establish the effects of directive antennas, to assess the isolation between co- and cross-polarized transmissions, to derive estimates of fade as well as non-fade durations, and to evaluate diversity reception. All these objectives have been met.

1. Background

Designing future mobile satellite systems, communication engineers require information on fade statistics associated with multi-path propagation in different types of terrain and shadowed line of sight transmissions due to roadside obstacles.

The objectives of earlier measurement campaigns [1 - 7] were to assess the statistics of fades under variable conditions: roadside obstacles, mountainous and flat terrain, elevation angles, side of roads and directions driven, seasonal effects, and unshadowed versus shadowed line of sight conditions.

The Australian campaign offered the opportunity to determine fade statistics for another continent having different types of foliage and terrain. It also enabled a broadening of a limited fade data base involving satellite platforms [5, 8, 9]. Transmissions from ETS-V were predominantly accessed, although signals emanating from the INMARSAT POR were also received. Major differences with previous data sets are: (a) high and low gain antennas were used, (b) transmissions from different satellites allowed probing fade variability with elevation angle, and (c) cross-polarization signals were measured during selected runs.

+ Mr. Hase was supported by a grant from the Science and Technology Agency of Japan during his 1988-1989 stay at The University of Texas as a visiting researcher.

In this effort we present fade statistics based on data selected from the campaign total of 1436 km road sampled, corresponding to 460 km of roads and encompassing 36 runs; a run representing a particular stretch of road with consistent parameters over which measurements were obtained and cataloged. Results pertaining to the following are exhibited: (1) fade distributions for different road types and differing densities of roadside obstacles (trees and utility poles), (2) overall average fade distribution and comparison with a previously derived empirical model, (3) fade distributions for different antenna patterns (high gain versus low gain), (4) fade distributions for different satellite transmitter platforms, (5) cross-polarization fade statistics, (6) fade and non-fade duration statistics, and (7) diversity gain improvement. Statistics associated with urban driving are not discussed, as terrestrial cellular systems are expected to be available at such locations.

2. Experimental Aspects

2.1 Transmitter and Antenna Systems

Left-hand circularly polarized (LHCP) CW transmissions radiated from the Japanese ETS-V satellite (EIRP = 55.9 dBm) were received at a frequency of 1545.15 MHz. Elevation angles ranged from 51° in Sydney to 56° in Coolangatta and the azimuth to the satellite was 2° counter-clockwise, relative to north. Although most of the selected measurements are for this satellite (28 runs, 446 km), measurements from INMARSAT POR (EIRP = 50 dBm, 10 runs, 68 km, RHCP, 1541.5 MHz, elev. 40°) are also included.

The low gain antennas were crossed drooping dipoles. The high gain antennas were manually pointed helixes (14 dB gain), thus restricting data acquisition to straight road sections.

2.2 Receiver and Data Acquisition System

Measurements were made with the Texas van receiver/data acquisition system. The receiver had three outputs with two noise bandwidths. Recorded were the in- and quadrature-phase detector voltages (bandwidth = 500 Hz), as well as the output from a power detector (200 Hz). The bandwidth was chosen because it did not exclude too many doppler-shifted multipath components when driving at highway speeds, yet retained a useful SNR for shadowing measurements.

Data were sampled at a 1 kHz rate and stored on magnetic disk in sequential records of 1024 samples. In addition to recording the L Band signals, the vehicle speed and time were also recorded.

The unfaded signal level was determined from the data itself. It was taken to be the mean level of the signal observed while driving in a location which produced minimal multi-path and

no shadowing. All the data reported are relative to that level. Only signal levels with at least 7 dB signal to noise are used.

2.3 Road Features

A map of the region indicating the rural roads outside the Sydney area traveled during the campaign is given in Figure 1. Measurements were made along these roads in non-contiguous blocks of about 30 to 70 km. Two major vegetation zones [10] were traversed in the experiment; forests (closed and open forms) along the coastal roads and woodlands (woodland and low-open woodland) further inland. Forests ranged from dry sclerophyll (most runs) to tropical rainforest (Run 385). The dominating tree genus in the forests was Eucalyptus. Other than tree types, more similarities than differences existed between apparent roadside conditions (tree heights, densities, setbacks) in Australia and the Eastern United States.

3. Fade Distribution Results

Fade levels are defined by 10*Log of the ratio of the measured power to the unfaded reference power. The distributions are presented with the ordinate depicting the percentage of the distance over which the attenuation exceeded the abscissa (fade) level. The distributions show fade levels from 0 to 20 dB over the probability range 1 to 100%. Low gain mode fades are calculated up to 15 dB and the high gain mode levels to 25 dB.

3.1 Worst Case Fade Levels

Consider the family of 15 fade distributions depicted in Figure 2. The runs are characterized as follows: (a) they were made in rural or suburban areas, (b) they all show fades due to trees and utility poles of 10 dB or more at the 1% probability, and (c) they represent measurements made with ETS-V in the low gain mode.

A physical interpretation relating the individual curves to specific roadside parameters is difficult; each road has varying densities of trees and utility poles along the sides with different setbacks, and also a variable local azimuth to the satellite due to bends in the roads. The worst case distribution in the set shown (Run 377) has an average 1:30 o'clock azimuth direction, but the road is winding along a small river and has large local direction changes. The many trees along this narrow road have only minimal setback and their branches frequently extend over the pavement. The smallest level fade distribution (Run 322) has an azimuth of 10:30, also in between the maximum and minimum shadowing geometry. The trees along this wide multi-lane road are not very close to its edge. We note that fades exceed values from 10 to 15 dB and 1 to 8 dB at the 1 and 10% probability, respectively.

3.2 Comparison with Empirical Roadside Shadowing (ERS) Model

In Figure 3 we have combined the distributions for the 15 individual runs of Figure 2 into a single distribution comprising 403 km of roads. Also plotted is the fade distribution as predicted by a model empirically derived from data obtained in the United States over 640 km [5], valid in the probability interval from 1% to 20%. The maximum difference between the two distributions is less than 2 dB at the 14% probability level. The ERS model has the following form:

$$F = -M * \mathrm{Ln}(P) + B \qquad (\text{for } 20\% > P > 1\%) \quad (1)$$

where the slope $$M = 3.44 + 0.0975*\theta - 0.002*\theta^2 \quad (2)$$

and the offset $$B = -0.443*\theta + 34.76, \quad (3)$$

and F is the fade depth exceeded in dB for P percentage of distance traveled. The angle θ is in degrees and corresponds to the elevation to the satellite. The model represents the average fade statistics for various road types with predominantly tree and some utility pole roadside obstacles. It includes different sides of the roads driven as well as different directions of travel. The model distribution in Figure 3 for $\theta = 51°$ is given by

$$F = -3.21 * \mathrm{Ln}(P) + 12.2 \; . \quad (4)$$

3.3 Distributions from Low and High Gain Receiving Antennas

Figure 4 illustrates a very heavy shadowing case. We note that the high gain antenna experiences consistently more fading than the low gain system, up to approximately 3 dB at 0.4% of the distance traveled. The attenuations for both antennas are due to a combination of tree absorption of the direct energy and scattering of energy out of and into the antenna beam. When the beam is narrower, less power is received via scattering. Conversely, the low gain, azimuthally omni-directional antenna receives more scattered multi-path contributions. Nevertheless, the higher gain antenna has 10 dB more gain and the net power received by it is still higher (7 dB more at 4% probability). For runs in which the line of sight was shadowed only occasionally, less than 1 dB fade differences existed.

3.4 Comparison of ETS-V and INMARSAT Measurements

Figure 5 is based on data taken over a 55 km tree lined road in the hills to the west of Sydney. This road was generally west-to-east, but made many turns in order to follow the contours of the landscape. Added into this figure have been the estimates of the median cumulative distribution functions predicted from the ERS model. For both satellites there is a tendency to overestimate fades below about 5 dB, but the error is less than

1 dB. The elevation angle dependence is well represented by the model.

4. Co- and Cross-Polarization Measurements

Figure 6 shows distribution functions for a pair of runs made sequentially along a rolling, suburban road lined with trees and utility poles, using high gain co- and cross-polarized antennas. The isolation between the two polarizations in the absence of nearby scatterers was better than 18 dB. Plotted are for Run 406 (copolarization) the percentage of the distance the fade exceeded the value on the abscissa and for Run 408 (cross-polarization) the percentage of the distance the fade was less than the abscissa. The horizontal distance between the curves gives an estimate of isolation between the two channels.

Since the data sets were not collected simultaneously, they cannot be used to determine the instantaneous polarization isolation. However, assuming that the occurrence of depolarization was highly correlated with shadowing, one can make reasonably accurate isolation estimates in the central range of percentages (about 10 to 60%). At the 10% level the fade values of 8 and 14 dB indicate an isolation of only 6 dB. The isolation is roughly inversely proportional to the fade threshold. Because of the random polarization of signals scattered by roadside obstacles, systems with any reasonable fade margin will not allow frequency re-use techniques.

5. Fade and Non-Fade Duration Statistics

From the viewpoint of designing an optimum system which transmits coded messages over designated bandwidths, it is important to know the length of time the land-mobile satellite channel is available and unavailable without interruptions. We have analyzed fade and non-fade duration distributions in order to determine the statistical characteristics of unavailability and availability, respectively.

5.1 Fade Duration

To reduce analyzing time and avoid effects of level crossings due to thermal noise, the original data were compressed by averaging over consecutive groups of eight samples. The resulting time series were quantized into two levels for each threshold examined, 2 to 8 dB at 1 dB increments. Durations have been expressed in units of distance traveled rather than in units of time, thus making them independent of the vehicle speed.

Cumulative distributions of fade durations are shown in Figure 7 for Run 383. Results were derived typical of suburban, rural, and heavy shadowing environments. Each of the many distributions could be represented by a log-normal, except at short durations of less than a wavelength (0.2 m). Contributions there are thought to be mainly due to level fluctuations caused

by the edges of obstacles. At 5 dB, all median values of duration are around 0.3 m except for the case of the high gain antenna, which has an average duration of about twice that value (0.63 m). All values of the slope are about 1.2 to 1.5 m, including the case of the high gain antenna. This means that they do not depend on either roadside or antenna parameters. Differences among the distribution curves for the various fade thresholds are small. For example, typical fade distance intervals at 1% are: 3..6 m, 4..8 m, 2..9 m, 7..10 m. Summarizing, fade durations measured in the low gain mode are shorter than those measured with a more directive antenna, but their slopes are similar.

5.2 Non-Fade Duration Analysis

Non-fade duration is defined as the continuous distance over which the fade levels are smaller than prescribed fade thresholds. A non-fade duration analysis of the data set above has been implemented using similar methods as those described for the fade duration analysis.

Typical results are shown in Figure 8. Unlike Figure 7, the ordinates in these graphs are scaled logarithmically. The cumulative distribution curves may be approximated by straight lines implying the exponential form,

$$P(d_n > x) = b\, x^{-c} \qquad (5)$$

where $P(d_n > x)$ is the percentage probability of the non-fade distance d_n exceeding the abscissa value x and where b and c are constants. The value of c, which is the slope in the graph, has a tendency to be larger for the heavier shadowing conditions. As this tendency is consistent for sufficient sample-size data, the value of c might be used as a quantitative measure of shadowing. Any difference due to threshold levels is small. Non-fade durations measured in the high gain mode are somewhat longer than those measured with the low gain antenna.

6. Phase Fluctuation Analysis

During the data analysis, phase data was extracted from the quadrature detected signals. Lower frequency components of the phase, mainly due to oscillator drift or doppler shift changes, were rejected by digital filtering. Distributions of the phase fluctuations under the condition that the received signal level is above a given fade threshold were determined. It was found that the deeper the fade threshold the larger the phase variance. Most distributions of phase fluctuations have such small variances that they will not affect a demodulator at all. Phase fluctuations with the high gain antenna are much smaller than those with the low gain antenna. This means that the influence of phase fluctuations to the demodulator can be ignored, except in the case of very heavy shadowing condition with the low gain

antenna. It is clear that the LMSS channel characteristics can be estimated by levels only, without any regard to phase.

7. Antenna Diversity Improvement

Above, it was shown that the average fade duration was of the order of 1 m, inspiring the test whether one could achieve significantly better performance of the MSS link if two antennas, separated in the direction of driving, were used instead of just one. The joint probability of the fade exceeding the threshold at two antennas was calculated for antenna separations of 1, 2, 5, and 10 m. Instead of using data collected with a second antenna, however, the original data was delayed by the time the vehicle needed to travel the separation distance. An example of the resulting family of fade distribution functions is shown in Figure 9. The diversity improvement factor DIF is defined by the ratio of the single antenna probability of failure P_0 to the joint probability of failure P_j and is a function of the fade margin. The overall result can be expressed by the relation

$$DIF = 1 + [0.2 * Ln(d) + .23] * F \quad (6)$$

where d (1..10 m) is the antenna separation in meters and F (3..15 dB) the fade margin in dB. For a separation of 2 m and a fade margin of 5 dB, for instance, a DIF of 2.8 results, meaning that a diversity system would fail in only less than half as many locations as a single antenna system. With longer separation (10 m) and a higher fade margin (10 dB) the DIF of 7.9 would indicate an even more dramatic improvement. For the analysis presented here, switching effects were not considered. An examination of the fade duration statistics with antenna diversity also showed that the number of fade events does not necessarily decrease, but that their average duration is reduced.

8. Summary and Conclusions

The Australian campaign has provided an enhanced MSS data base of propagation information associated with shadowing, multipath, antenna directivity, and cross polarization due to roadside obstacles for various road types. The results described here complement those acquired via satellite measurements in the U.S., Canada, and Europe and provide information as to the characteristics of fade statistics in a different continent.

We conclude the following from the results:

(a) The fade statistics due to roadside trees and utility poles along rural or suburban roads in Australia are typical of those in the U.S. with similar densities of roadside obstacles.

(b) The overall average fade distribution was found to agree with the fade distribution predicted by the ERS model within 2 dB and less over the probability range of 1% to 20%.

(c) The employment of directive antennas for the severe shadowing condition resulted in more fading than with a less directive system. Although there is a fade increase for the more directive system, this is more than offset by the significant gain improvement for the system. Another advantage of the high gain antenna is the fact that the non-fade duration is longer.

(d) Comparison of fade distributions along the same section of roads employing the ETS-V and INMARSAT POR satellite transmitter platforms demonstrated the ERS model scales well with elevation angle.

(e) Frequency reuse does not appear to be a viable option for MSS communications, since depolarization due to obstacles in the vicinity of the line of sight reduces the isolation to unacceptable levels.

(f) Fade duration cumulative distributions may be approximated with log-normal fits. The fade duration expressed in m of travel has been shown to be relatively invariant to the threshold fade level. Typically, fade durations at 1% probability range from 2 to 8 m. For runs exhibiting more shadowing, fade durations are about 7 to 10 m at 1% probability. This is approximately consistent with fade duration statistics acquired in the U.S. for similar fade conditions [4].

(g) Non-fade duration cumulative distributions may be described with good accuracy by power curve fits where the exponent of the non-fade duration distance is representative of the extent of roadside shadowing. When it is approximately 0.75 or larger, heavy shadowing is prevalent. Lighter shadowing cases result in c in the range of 0.5 to 0.6.

(h) Phase fluctuations are generally so small that the channel characteristics can be estimated from the levels only.

(i) Employing two antennas on the vehicle to obtain diversity improvement, the fraction of the roads along which MSS is faded into inoperability can theoretically be reduced by a factor from 2 to 8. It may be difficult to achieve this improvement in a real system, however, when the effects of switching cannot be neglected.

9. Acknowledgements

The authors are grateful to AUSSAT for sharing in the costs of this experiment and to AUSSAT's Mobilesat group for invaluable logistical and technical support during the campaign. Many thanks are also extended to the Japanese Government for providing the satellite transmissions of ETS-V. We also acknowledge INMARSAT for enabling measurements with INMARSAT POR. This work was supported by the Jet Propulsion Laboratory for the University of Texas under Contract JPL956520 and by NASA Headquarters, Contract #N00039-89-C-5301 for APL.

References

[1] Vogel, W. J. and J. Goldhirsh, "Tree Attenuation at 869 MHz Derived from Remotely Piloted Aircraft Measurements," IEEE Trans. on Antennas and Propagation, AP-34, No. 12, pp. 1460-1464, December 1986.

[2] Goldhirsh, J. and W. J. Vogel, "Roadside Tree Attenuation Measurements at UHF for Land-Mobile Satellite Systems," IEEE Trans. on Antennas and Propagation, APS-35, pp. 589-596, May, 1987.

[3] Vogel, W. J. and J. Goldhirsh, "Fade Measurements at L Band and UHF in Mountainous Terrain for Land Mobile Satellite Systems," IEEE Trans. on Antennas and Propagation, APS-36, January, 1988.

[4] Goldhirsh, J. and W. J. Vogel, "Mobile Satellite System Fade Statistics for Shadowing and Multipath from Roadside Trees at UHF and L Band," Accepted for publication in IEEE Transactions on Antennas and Propagation, April 1989.

[5] Vogel, W. J. and J. Goldhirsh, "Mobile Satellite System Propagation Measurements at L Band Using MARECS-B2,". To be published at future date in IEEE Transactions on Antennas and Propagation (Accepted for publication 4/89).

[6] Goldhirsh, J. and W. J. Vogel, "Propagation Degradation for Mobile Satellite Systems," Johns Hopkins University, Applied Physics Laboratory Technical Digest, April-June 1988, Volume 9, Number 2, pp. 73-81.

[7] Vogel, W. J. and Ui-Seok Hong, "Measurement and Modeling of Land Mobile Satellite Propagation at UHF and L Band," IEEE Trans. on Antennas and Propagation, Vol. AP-36, pp. 707-719, May 1988.

[8] Butterworth, J. S., "Propagation Measurements for Land-Mobile Satellite Systems at 1542 MHz," Communications Research Centre, Ottawa, Canada, Tech. Note No. 723, August 1984.

[9] Jongejans, A., A. Dissanayake, N. Hart, H. Haugli, C. Loisy, and R. Rogard, "PROSAT - Phase 1 Report, European Space Agency Technical Report ESA STR-216, May 1986 (European Space Agency 8-10 Rue Mario-Nikis, 75738 Paris Cedex 15, France)

[10] Dept. of Arts, Heritage and Environment, Think Trees Grow Trees, Australian Government Publishing Service, Canberra, 1985

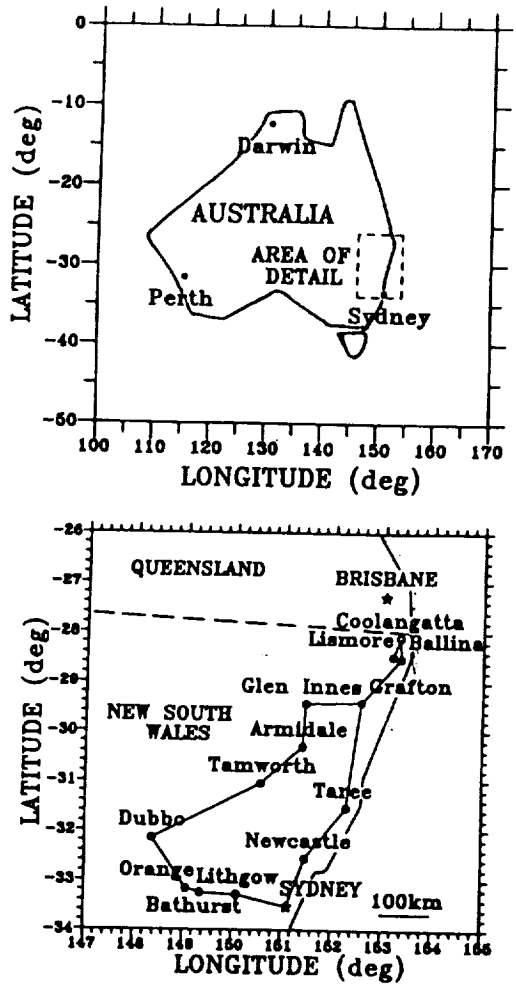

Fig. 1 The roads of South-East Australia along which measurements were taken during campaign.

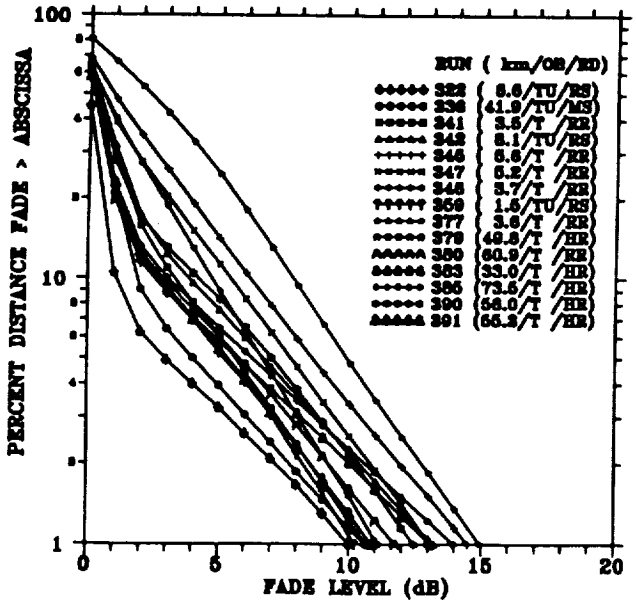

Fig. 2 Fade distributions for all tree and utility pole runs.

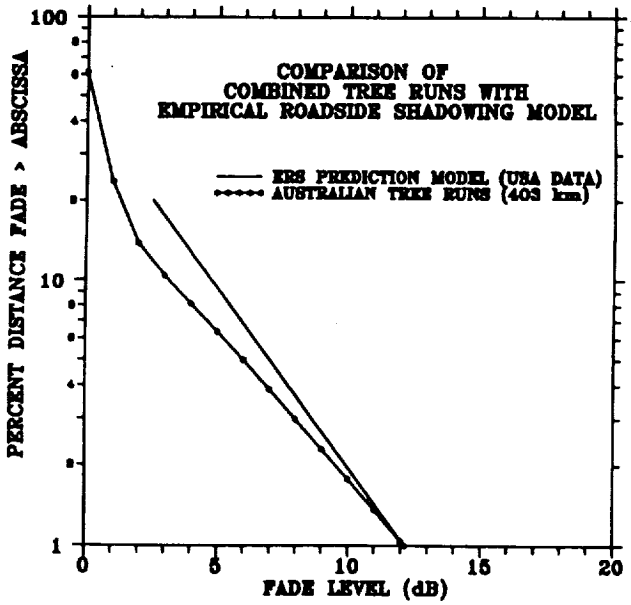

Fig. 3 Combined tree runs compared to USA derived ERS model.

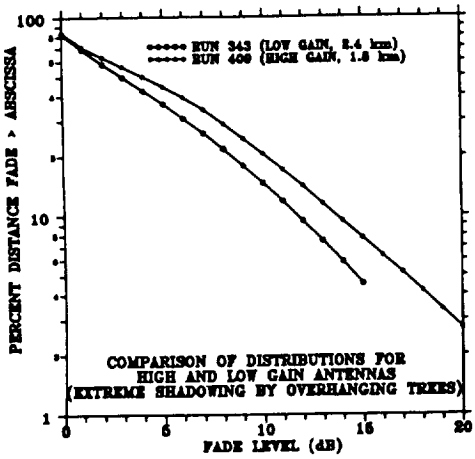

Fig. 4 Comparison of high and low gain antenna measurements under extreme shadowing.

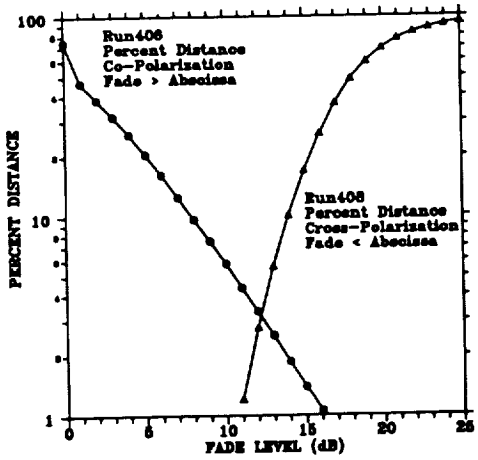

Fig. 6 Estimated cross polar isolation of high gain antenna.

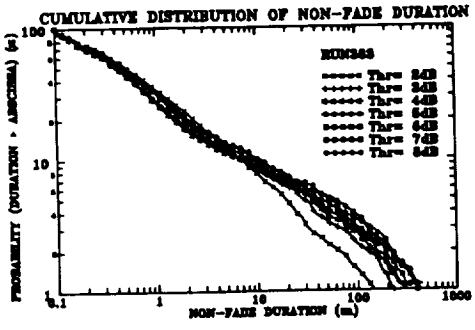

Fig. 8 Cumulative distribution of measured non-fade durations.

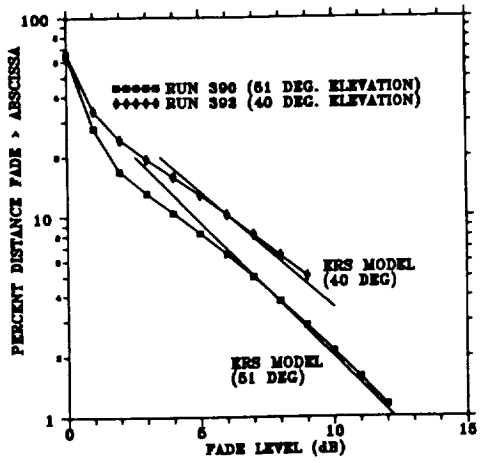

Fig. 5 Elevation angle scaling of ERS model and data from ETS-V and INMARSAT POR.

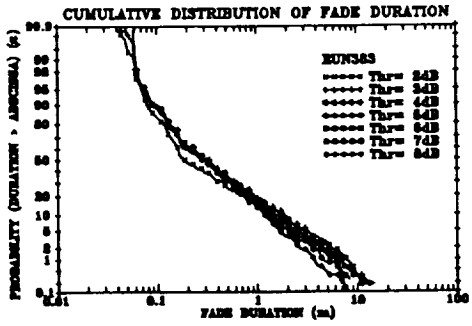

Fig. 7 Cumulative distribution measured fade durations.

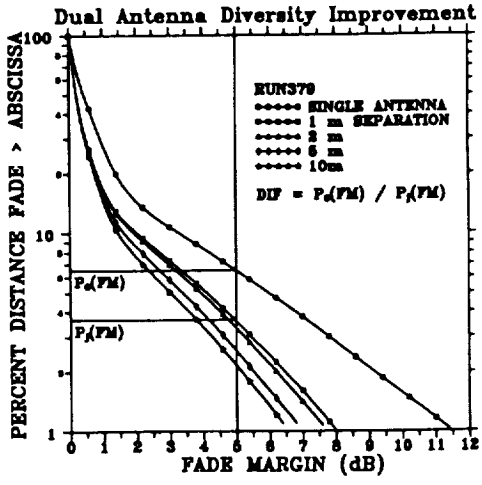

Fig. 9 Diversity improvement as a function of antenna separation.